ND TESTING ADVANCES ON CFRP WITH ULTRASONIC AND THERMAL TECHNIQUES

A. Carofalo[1], V. Dattoma[1], F. Palano[1]*, F.W. Panella[1]

[a] *Department of Engineering for Innovation, University of Salento, Lecce, Italy*
** Corresponding author* (fania.palano@unisalento.it),

Keywords: thermographic analysis, Composites, CFRP plates, ND Testing, Ultrasonic analysis, artificial defects.

Abstract
Purpose of the job is to perform measurements on two specimens with ND control procedures on composite material with carbon fibers and different thickness, containing artificial defects similar in shape, but with different typology, in order to allow the detection tests to be adapted on large and small defects at certain depths.
The analysis was performed using the Thermography Pulsed technique and Phased Array ultrasonic inspection, comparing the detection of artificial defects of different sizes and different typology, identified at different depths as with the real ones. All the important factors that enable the success of a scanning method with ND controls were studied, allowing to evaluate the efficacy of the used techniques and tools in the studied cases.

1. Introduction

The objective of this work is to perform non-destructive testing on modern laminates in carbon fiber/epoxy resin of high technological quality, since derived from aeronautical production, studying the performance of pulsed thermography and ultrasonic phased array technologies to identify defects. Two specimens were assembled with artificial defects: two plates of different thicknesses are glued and the defects are created in between with the intent to simulate delaminating defects. In the first plate the defects are filled with air, while in the second are filled with expanded polystyrene; defects are positioned according to the same scheme and some defects were placed near the side of the specimen in order to observe the edge effects. Furthermore, the defects present different sizes to evaluate the influence of dimension, depth and thickness on their detection possibility.

1.1. Typical defects of CFRP

The failure behavior of CFRP parts is connected to the growth of cracks, whose formation is due to manufacturing defects, such as micro voids, micro-cracks in the matrix, or delamination in service phenomena. The most dangerous are the micro voids and delaminations which degrade significantly the mechanical properties, especially in case of fatigue stresses: in fact, when the number of cycles raise an increase of the delaminated area can be observed, whilst the most common cause of micro voids presence is the inability of the resin to expel the air from the surface from liquid resin during curing phases [1-2].

2. Material and Methods

The information in terms of thermal conductivity and density of the CFRP constituents are shown in table 1 [4-5].

Parameters	Carbon fibre	Epoxy resin
Density	1.65 [g/cm^3]	1.13 [g/cm^3]
Areal weight	240 [g/m^2]	
Thermal conductivity coef.	~15 [W/mK]	~0.22 [W/mK]

Table 1. Properties of constituents materials.

2.1. Tested specimen

Two different specimens with artificial defects were produced, the three original plates consist in laminates with symmetric lamina oriented ±0/90°, coupled with ±45°at borders with different thicknesses; defects have the intent to simulate delaminating. In the first plate the defects are filled with air, while in the second are filled with expanded polystyrene. In both plates the defects are positioned according to the scheme in fig.1. Furthermore, different sizes of defects are created to evaluate the influence of their size, depth (different if measured from the opposite sides) and thickness on the possibility of their detection.

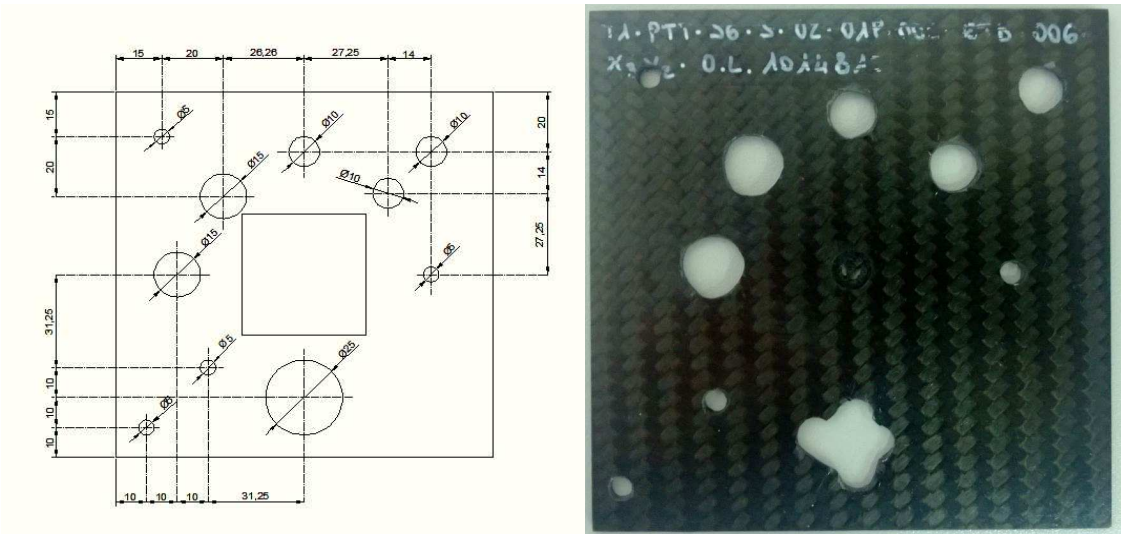

Figure 1. Drawing of artificial defects position, manually worked on internal laminate.

2.1.1 Specimen A

The specimen has been realized through bonding of three square laminates of side 172 mm with different thicknesses, of which the central one is perforated according to the design constructive reported (fig.2). The thicknesses of the single laminates are respectively 2.8 mm (8 layers) and 2.1 mm (6 layers) for a total of 7 mm. The specimen allows to analyze defects of elevate thickness. Defects with different sizes were created to study the relationship

between the detection of a defect and its size and depth (fig.3 and table 2). Some holes, such as D9, D6 and D7, were placed in order to study the thermal detection at the plate edges. In addition, a warmer area will be observed at the thermal center of the plate to due to an existing hole, whose existence is due to the use of these laminates in previous experimental works.

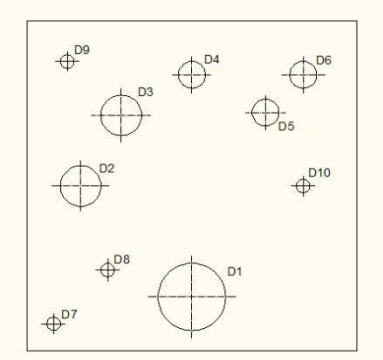

Figure 2. Designation and position of defects

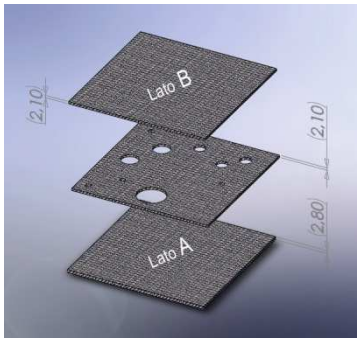

Figure 3. Structure of specimen A

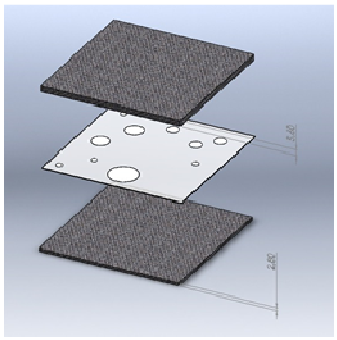

Figure 4. Structure of specimen B

Dimension	Designation
$\phi 5$	D7, D8, D9, D10
$\phi 10$	D4, D5, D6
$\phi 15$	D2, D3
$\phi 25$	D1

Table 2. Dimension of artificial defects.

2.1.2 Specimen B

The specimen B (Fig.4), has been made through the bonding of two square laminates with different thicknesses and circular disks of polystyrene foam were inserted between, arranged as in the constructive drawing shown above. The thickness of the laminates are 2.8 mm (8 sheets) and 5.6 mm (16 sheets) for a total of 8.4 mm. The material of the specimen is always the same as for specimen type A. During the manufacturing the precise location of defects does not respect the arrangement of the constructive drawing: this is due to the fact that the disks of polystyrene can slightly move during the bonding operation. The aim of this second specimen is to verify the possibility to analyze artificial defects of the same nature but with a much less thickness.

2.2. Non Destructive Technique

The Non-destructive testing (NDT) methods are very simple and in most cases do not require any physical contact between the equipment and the analyzed object and allow not to damage the parts, ensuring a well-functioning of the analyzed surfaces. These techniques can also be applied during the production phase and the great advantage is the detection of defects also on large surfaces. Nowadays the most common non-destructive techniques for composites are the Ultrasound and Thermography techniques.

2.2.1 Thermographic Inspection procedures

Thermography is a non-destructive inspection techniques that allow the detection of defects in aerospace CFRP parts [1,6]. The advantages of this control is the speed of acquisition data and the low risk of specimen damage of the analyzed.
The main equipment tool for this technique is the infrared detector, a sensor capable to convert the radiant energy into an electrical signal. Pulsed Thermography consists in a shortc in time heating phase of the specimen, followed by the analysis of thermal frames during the cooling phase. The presence of a defect in a thermogram is detected in a temperature-time diagram comparison between the curve of thermal performance of a defect zone with a reference not defected surface to be observed. To better evaluate defect thickness and diameter, a thermal contrast evaluation on the flaw area is necessary. In this study the absolute contrast and normalized contrasts are defined as:

$$C_a(t) = T_d(t) - T_i(t) \quad (1)$$

$$C_n(t) = \frac{T_d(t)}{T_d(t_0 + 1)} - \frac{T_i(t)}{T_i(t_0 + 1)} \quad (2)$$

where T is the temperature, t is the time instant chosen, while the subscripts d and i refer to a defected and no-defected area; t_0 is the instant when the heating ends. A thermal imaging camera FLIR SC7000 model with tripod is used, with a resolution NETD (Noise Equivalent Temperature Difference) of 20 mK; two halogen lamps with a 2 KW maximum power generate heat input flux on the specimen surface. In reflection Pulsed techniques, the camera is centered between the two lamps in front of the illuminated surface of the specimen [2]; therefore, the camera is positioned at a fixed distance of 35 cm from the lamps and at different distances from the specimen, between 80 cm and 35 cm.

2.2.2 Ultrasounds Inspection

Ultrasonic waves are an example of mechanical waves, whose disturbance propagates through solid medium. The ultrasonic signal is generated by piezoelectric materials and thanks to the action of an electric field with appropriate frequency.
The ultrasound probe waves are emitted in the material to be analyzed, placing the transducer on the surface. A coupling system is placed between the material and the probe to reduce the absorption of the signal, generally water or gel based creams. In this work the pulse/echo technique is applied, allowing to identify defect characteristics (size and geometry).
The used device is the Olympus Omniscan MXU, while an innovative technological 16 X 16 elements Phased Array (PA) probe is used.
The Phased Array system uses the physical principle of multiple progressive waves, varying the time between a series of ultrasonic pulses, so the wavefront generated by each element of the array at slightly different times combines with anothers to direct and shape the sound beam and achieve a sharp focus and different beam direction.
The PA system can transmit an ultrasound beam through a series of angles of refraction or along a linear path, or dynamically focus different depths, thus increasing the flexibility and the ability of control procedures.
The scan operation was done by splitting the specimen into regular strips of constant amplitude (about 10 mm) and using a Mini-Wheel™ encoder, which is connected to the probe, to synchronize the probe data acquisition with the probe unidirectional motion. The scans are displayed on C-scan diagrams, which present a two-dimensional view of data displayed in a top or planar view on specimen, monitoring the data in the XY position. The

defects size or depth indications are obtained for a given gain tuning from the values on the horizontal axis of the C-scan

3. Results and discussion

3.1 Themographyc tests analysis

After first tests determined by previous warm-up time experimentations, three tests were performed with different heating times (5 s, 10 s, 15 s) on the surface of specimen A with thickness 2.8 mm. The distance between specimen and the camera is optimized at 80 cm and 88 cm from the lamps. The defects D1, D2, D3, D4, D5 and D6 are easily visible (Figure 5), while the defects D7, D8, D9 and D10 are not visible in the thermal test. For the opposite surface (2.1 mm) .

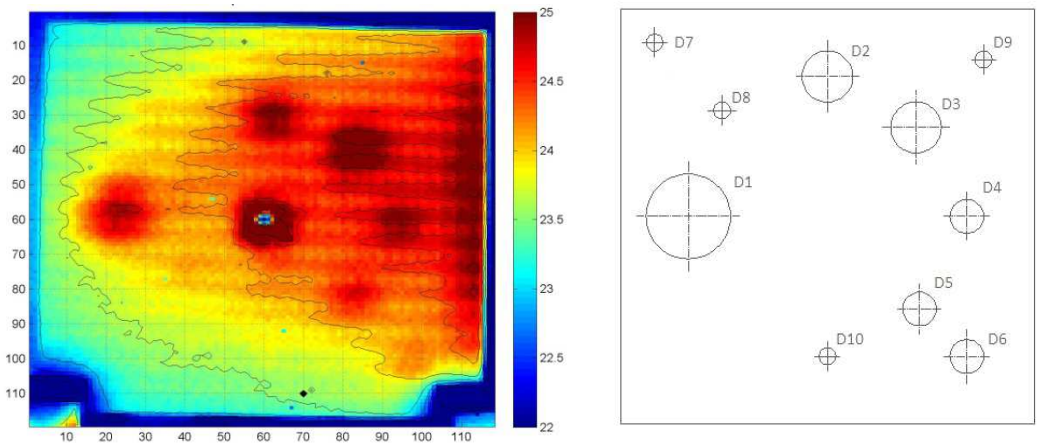

Figure 5. Thermograms obtained after 8 cooling seconds after heating pulse of 10 s, compared with correct position scheme of artificial defects.

The optimal heating times were different (3 s, 7 s, 12 s and 17 s). The defects D1, D2, D3, D4, D5 and D6 are evident (Fig. 6) with the defect D8 only with heating times 7 s and 12 s. So the heating time necessary for a good resolution of defect indications is found to be 7 s. Therefore, it is conceivable that the optimal selected heating time is directly proportional to the depth of the defect.

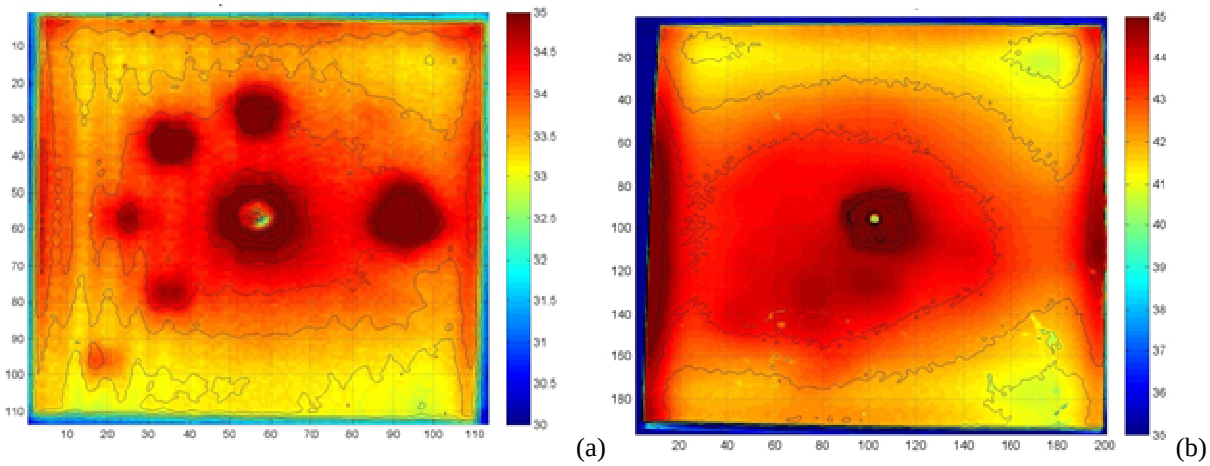

(a) (b)

Figure 6. Thermograms obtained after 7 s cooling seconds after heating pulse on the 2.1 mm laminate side (distance 80 cm between the specimen and camera) and original defect positions. (b) Thermograms obtained after 7s on the 2.8 mm laminate side (distance 30 cm between the specimen and camera)..

In the B specimen, containing artificial defects in expanded polystyrene, the tests with 8s and 10s long heating pulses allowed to identify four defects (Fig. 6a) in analogy with Figure 5. These tests were performed to evaluate if a further reduction of the camera/specimen distance corresponds to an improvement of the defect resolution, in case a reduction of the heating times is desired. Two more tests with the same equipment arrangement were performed, but with a distance specimen/lamps of 30 cm and reducing the distance between the lamps from 66 cm to 50 cm (fig.6b). Similar results are measured in other configurations and are hereby omitted.

3.2 Phased Array ultrasonic tests results

The phased array scanning experiments were executed on both of specimens A and B. Measurements were done on both sides of specimens to verify the technique at different depths. Table 3 shows the resulting amplitude data for each individual defect as detected for both scans after optimal measurements were achieved, with the value of the real size of the defect, the signal peak value and the measured dimensions, imposing a signal reference value, which represent a color value (yellow) referred to the presence of defects, equal to 60 dB, for the 6 layers side and 50 dB for the 8 layers side (fig.7).

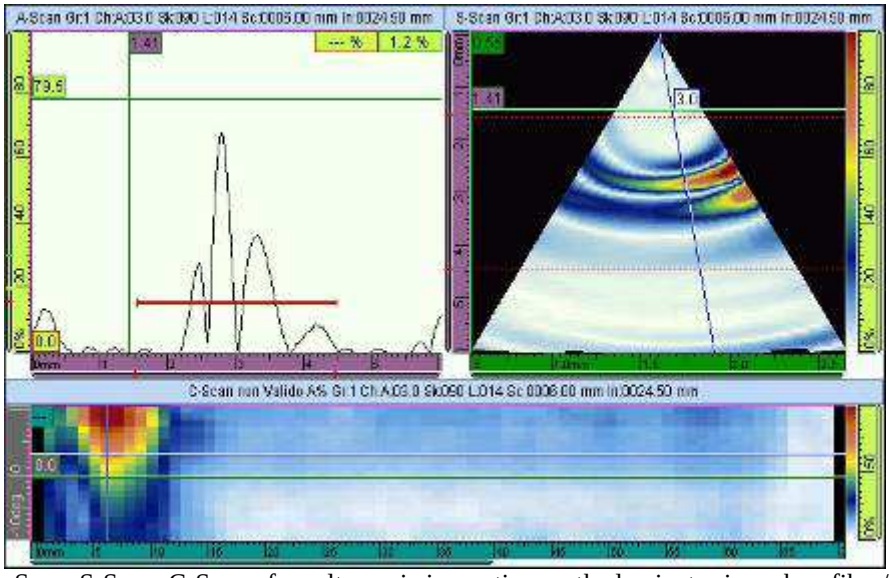

Figure 7. A-Scan, S-Scan, C-Scan of an ultrasonic inspection on the laminates in carbon fiber/epoxy resin containing artificial defects in expanded polystyrene.

All defects of any size is proved to be detectable with the Phased array technology for a depth of 2.1 mm, while at 2.8 mm there is a decay of the reflected beam signal, which allows to identify only larger defects (from 10 mm upwards), with poor and unreliable results for smaller defects.
Table 4 instead, shows the results referred to B type specimen, with defects generated by polystyrene diskettes, sandwiched between two carbon fiber plates of different thickness. Depth for defects and shape is similar to specimen type A. The amplitude of the measured signal never reaches the level of 60 dB as in the previous case, so a reduced threshold value of 40 dB was established. In this analysis and at 2.8 mm of depth, the technique allows to detect the defects larger than 10 mm in diameter, but with and observed peak underestimation of about 5% with respect to case A, while the defects with a minor diameter are not clearly detected or invisible at all and strongly underestimated.

Defect	Real dimensions [mm]	Amplitude [dB]	Estimated Size [mm]	Difference [%]
D1	ϕ 25	> 100	25	100%
		96	24.6	98.4%
D2	ϕ 15	> 100	15	100%
		100	14.8	98.67%
D3	ϕ 15	> 100	15	100%
		79.5	14.8	98.67%
D4	ϕ 10	100	9.8	98%
		63	9.8	98%
D5	ϕ 10	100	10	100%
		83	10	100%
D6	ϕ 10	100	10	100%
		52	9.8	98%
D7	ϕ 5	38	5	100%
		30	N.A.	0%
D8	ϕ 5	42	5	100%
		40	3.2	64%
D9	ϕ 5	48	5	100%
		50	N.A.	0%
D10	ϕ 5	25	N.A.	0%
		24	N.A.	0%

Table 3. Results of scan on specimen A

For a depth of 5.6 mm the technique shows a detection capability suitable only for large defects, 15 mm in diameter , whilst for smaller defects the dispersion of the beam is elevated, even with a probe of 4 MHz and is impossible to identify clearly any significative change in the signal response with respects to surrounding sound area; in particular the measurements in these cases are found to be confused with background noise and affect a correct diagnosis.

Defect	Real dimensions [mm]	Amplitude [dB]	Estimated Size [mm]	Difference [%]
D1	ϕ 25	70	24.8	99.2%
		50	23	92.%
D2	ϕ 15	60	14.7	98.%
		41	14	93.33%
D3	ϕ 15	58	13.7	91.33%
		41	12	80%
D4	ϕ 10	63	9.8	98%
		30	N.A.	0%
D5	ϕ 10	47	9.7	97%
		34	N.A.	0%
D6	ϕ 10	56	9.8	98%
		36	N.A.	0%
D7	ϕ 5	40	3.6	72%
		32	N.A.	0%
D8	ϕ 5	40	2.7	54%
		20	N.A.	0%
D9	ϕ 5	33	N.A.	0%
		32	N.A.	0%
D10	ϕ 5	24	N.A.	0%
		28	N.A.	0%

Table 4. Results of scan on specimen B

Conclusions

The performance of pulsed thermography and ultrasonic phased array technologies as ND control tools were analyzed, if applied to modern CFRP plates for aeronautical applications. Artificial defects of different shape, thickness and depth were built in two different stacking ways and several scanning measurement were accurately performed to optimize defects detection. Results show both techniques are valid, even that UT methods seems to offer better results.

References

[1] P.K. Mallick, *Fiber-Reinforced Composites: Materials, Manufacturing and Design*, 2nd ed. revised and expanded, Cap 2, pag 15-55, New York, 1993;

[2] G. Wróbel Z. Rdzawski G. Muzia S. Pawlak, , *The application of transient thermography for the thermal characterisation of carbon fibre/epoxy composites*, Journal of Achievements in Materials and Manufacturing Engineering, Volume 36 Issue 1 (2009);.

[3] U. Gallietti L. Spagnolo D. Palumbo, *Tutorial on the Thermography*, Department of the Mechanical Engineering, Politecnico di Bari, Italia.

[4] Jawdat Tashan Riadh Al-mahaidi, *Investigation of parameters that influence the accuracy of bond defect detection in CFRP bonded specimens using IR thermography*, Composite Structures 94, 519–531, 2011.

[5] C. Goidescu H. Welemane C. Garnier M. Fazzini R. Brault El. Péronnet S.Mistou, *Damage investigation in CFRP composites using full-field measurement techniques combination of digital image stereo-correlatio, infrared thermography and X-ray tomography*, Composites: part B 48, 95-105, 2012;

[6] M. Susa X. Maldague I. Boras, *Improved method for absolute thermal contrast evaluation using Source Distribution Image (SDI)*, Infrared Physics & Technology, 53, 197–203, 2010.